The number of PML nuclear bodies increases in early S phase by a fission mechanism

Graham Dellaire*, Reagan W. Ching*, Hesam Dehghani‡, Ying Ren and David P. Bazett-Jones§

Programme in Cell Biology, The Hospital for Sick Children, 555 University Avenue, Toronto, Ontario, M5G 1X8 Canada

*These authors contributed equally to this work

‡Present address: Department of Physiology, School of Veterinary Medicine, Ferdowsi University of Mashhad, Mashhad, Iran

§Author for correspondence (e-mail: dbjones@sickkids.ca)

Accepted 30 November 2005
Journal of Cell Science 119, 1026-1033 Published by The Company of Biologists 2006
doi:10.1242/jcs.02816

Summary

Promyelocytic leukemia (PML) nuclear bodies have been implicated in a variety of cellular processes including apoptosis, tumour suppression, anti-viral response, DNA repair and transcriptional regulation. PML nuclear bodies are both positionally and structurally stable over extended periods of interphase. As demonstrated in this study, the structural stability is lost as cells enter S phase, evidenced both by distortions in shape and by fission and fusion events. At the end of this period of structural instability, the number of PML nuclear bodies has increased by a factor of twofold. Association of the fission products with chromatin implies that the PML nuclear bodies respond to changes in chromatin organisation or topology, and thus could play a role in monitoring genome integrity during DNA synthesis or in the continued maintenance of functional chromosomal domains prior to mitosis.

Supplementary material available online at
http://jcs.biologists.org/cgi/content/full/119/6/1026/DC1

Key words: PML nuclear body, DNA synthesis, Electron spectroscopic imaging, Particle tracking, Nuclear organisation

Introduction

The promyelocytic leukaemia (PML) protein, a member of the RING-finger family of proteins, is implicated in a number of cellular processes including transcriptional regulation, tumour suppression, apoptosis, DNA repair and the replication of both viral and cellular DNA (Bernardi and Pandolfi, 2003; Dellaire and Bazett-Jones, 2004; Everett, 2001). In normal cells, the PML protein is found in 5-30 sub-nuclear domains of approximately 0.3 to 1 μm in diameter, which are known as PML nuclear bodies (Melnick and Licht, 1999). During extended periods in interphase, PML nuclear bodies are quite immobile and appear to maintain their relative positioning through extensive contacts with the surrounding chromatin (Eskiw et al., 2004; Eskiw et al., 2003; Wiesmeijer et al., 2002). By contrast, these bodies are highly dynamic following heat or heavy metal shock and in response to DNA damage. These cell stresses lead to the breakdown of PML nuclear bodies by fission of supramolecular assemblies of PML from the parental bodies (Eskiw et al., 2004; Eskiw et al., 2003). Indeed, PML nuclear body integrity and dynamics are intimately linked to the state of chromatin organisation in the cell, and these structures appear to act as sensors of cellular stress (Dellaire and Bazett-Jones, 2004).

PML nuclear bodies may also represent sites of specific nuclear events such as DNA transcription, replication and repair. For example, transcriptionally active chromosomal domains (Wang et al., 2004) are found to preferentially associate with PML nuclear bodies. Sites of nascent DNA synthesis have also been reported to associate with these structures in mammalian cells. Following DNA damage several DNA repair factors transit to and from PML nuclear bodies and the bodies themselves have been found to colocalise with sites of unscheduled DNA synthesis in damaged cells, implicating these bodies in DNA repair (Dellaire and Bazett-Jones, 2004). Therefore, rather than serving as passive depots for nuclear proteins, these studies support a central role for PML nuclear bodies in the DNA metabolism of mammalian cells.

The number and size of PML nuclear bodies can vary dramatically between cell and tissue types. Whereas levels of expression of PML protein affect the size of bodies, the number of bodies can be related to chromosomal ploidy (Chang et al., 1995; Drouin et al., 2001) and whether cells are cycling (Koken et al., 1995; Terris et al., 1995). Since PML nuclear body integrity is dependent on chromatin (Eskiw et al., 2004) and their numbers are related to chromosomal ploidy, we wished to address the effect of DNA replication on PML nuclear body structure. Using both electron microscopy (EM) and live-cell imaging, we report that the structural stability of PML nuclear bodies is compromised in early S phase, evidenced by distortions in shape and position of the bodies by live-cell microscopy and by EM. These changes in PML nuclear body integrity eventually result in body fission, producing PML microbodies that are biochemically similar to the parental bodies. These structures exhibit constrained diffusion similar to that of chromatin. Their association with chromatin was confirmed by correlative light microscopy and EM. Although the ultrastructure of some microbodies is truly body-like in appearance as suggested by light microscopy, by EM a subset exists as protein structures that appear to coat chromatin fibres. When S phase is complete, the net increase in number of PML nuclear bodies is approximately twofold, depending on the cell type. We suggest that PML nuclear body dynamics and integrity in S phase is a reflection of changes in chromatin topology as DNA is replicated. These data provide evidence

for a more intimate and dynamic link between PML nuclear body integrity and chromatin in the interphase cell than previously appreciated. We discuss the implications of this discovery for models of nuclear organisation and PML nuclear body function.

Results

PML nuclear body number increases upon entry into S phase

To explore a possible relationship between PML nuclear body number and the cell cycle, we followed living human SK-N-SH neuroblastoma cells by differential interference contrast (DIC) microscopy for 18 hours prior to fluorescence imaging. We correlated the time post cytokinesis with DNA content (DAPI), PML nuclear body number and cyclin A levels (immunofluorescence) (Fig. 1A). During the first 3 hours of S phase, as determined by increasing cyclin A levels (Erlandsson et al., 2000), PML nuclear body number increased dramatically. Twelve hours post cytokinesis the DNA and cyclin A levels continued to rise before reaching a plateau at 16 hours, whereas the PML nuclear body number remained constant during this time. The number of PML nuclear bodies increased by approximately twofold (i.e. ratio of PML nuclear body number in G2 versus G1), a result obtained with other cell lines as well, including human primary skin fibroblasts (GM05757) and U-2 OS human osteosarcoma cells (data not shown).

To confirm with better temporal resolution that PML nuclear body number increases in early S phase, U-2 OS cells stably expressing GFP-tagged PML IV were synchronised at the G1-S-phase border with aphidicolin before being released into S phase (Fig. 1B). Efficient synchronisation and release into S phase was monitored by fluorescence activated cell sorting (FACS) analysis (data not shown). PML nuclear body number averaged over 40 cells increased very rapidly in the first hour after aphidicolin release and reached a plateau between 2 and 3 hours post release. This experiment was repeated using normal U-2 OS cells to ensure that the increase in PML nuclear body number was not due to the overexpression of GFP-PML IV. As shown in supplementary material Fig. S1, the kinetics of PML nuclear body formation in S phase in U-2 OS cells were similar to those observed in U-2 OS cells expressing GFP-PML IV (Fig. 1B), and therefore indicate that the increase in PML nuclear body number observed in the synchronisation experiments is not due to the overexpression of PML. To visualize the changes in PML nuclear bodies within a single cell during S phase, U-2 OS GFP-PML IV cells were synchronized and individual cells were imaged every 5 minutes for 5 hours (supplementary material Fig. S2). Within an individual cell, the number of PML nuclear bodies fluctuated

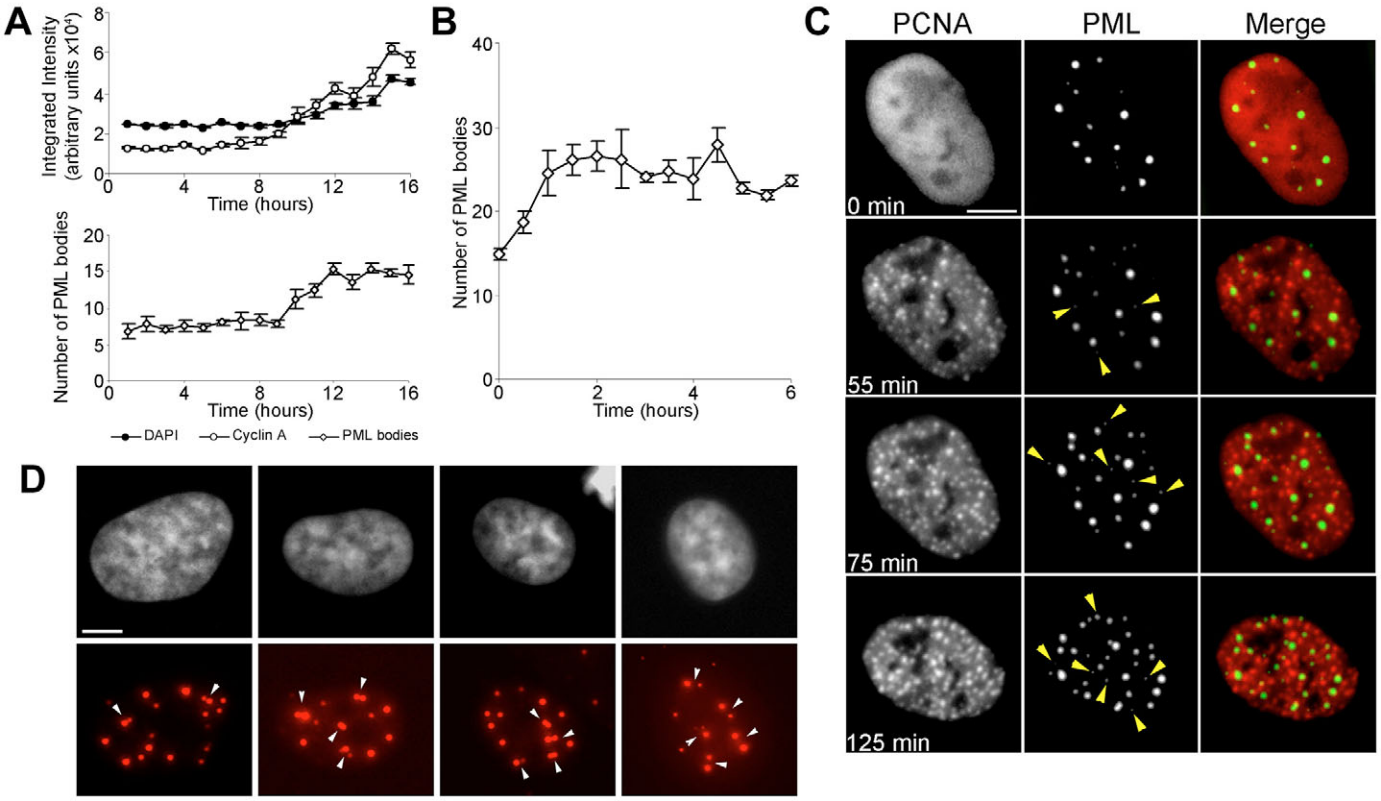

Fig. 1. PML nuclear bodies increase in number during S phase. (A) Asynchronous human SK-N-SH cells were followed by DIC to determine relative cell cycle position after mitosis over an 18 hour period prior to immunolabelling for cyclin A. (B) Human U-2 OS cells stably expressing GFP-PML IV were synchronised at the G1-S border with aphidicolin and released into S phase for 2-6 hours. PML nuclear body number versus time is shown. (C) Asynchronous U-2 OS cells expressing diHcRed-PCNA (PCNA) and GFP-PML IV (PML) were observed for 2 hours by spinning-disk confocal microscopy. Images shown are compressed *z*-stacks. Newly replicated PML nuclear bodies are indicated by yellow arrowheads. (D) PML nuclear body doublets are present in SK-N-SH cells in mid S phase (arrowheads). Bars, 5 μm.

as cells progressed though S phase, but increased in number for approximately 200 minutes, after which the number remained constant. This is consistent with the behaviour averaged over many cells (Fig. 1A,B). The fluctuation in PML nuclear body number in individual cells suggests that PML nuclear bodies are fissioning and fusing, but with a greater propensity to fission. To ensure that entry into S phase was primarily responsible for the dramatic increase in PML nuclear body number, rather than an indirect result of the synchronisation method, asynchronous U-2 OS cells expressing both diHcRED-PCNA and GFP-PML IV were followed by live-cell microscopy for several hours (Fig. 1C). The distribution pattern of the PCNA protein changes during the cell cycle, appearing diffuse in G1 and as punctate foci in S phase (Leonhardt et al., 2000). Therefore, this change in PCNA distribution pattern provides a reliable marker for entry into S phase. In agreement with data obtained from synchronised cells, we observed the accumulation of new PML nuclear bodies in asynchronous U-2 OS cells during early S phase (Fig. 1C).

Since new PML nuclear bodies might arise from new protein synthesis in S phase, we analysed the levels of PML protein in the normal human fibroblast line GM05757 during the cell cycle by quantification of both immunofluorescence detection of PML and western analysis (supplementary material Fig. S3). The highest levels of PML protein are found in G1 and these levels drop by as much as 10 and 30 percent in S phase and G2, respectively. We conclude that the increase in PML nuclear body number in early S phase is not a function of increasing PML protein levels.

PML nuclear bodies become structurally unstable and divide by a fission mechanism in early S phase

We demonstrated previously that the structural integrity of PML nuclear bodies is maintained by chromatin contacts and is affected by changes in the degree of condensation and integrity of chromatin (Eskiw et al., 2004). We therefore hypothesised that changes in DNA topology or loss of chromatin contacts with PML nuclear bodies may also lead to structural instability. To address this, we observed synchronised GFP-PML IV expressing U-2 OS cells as they entered S phase. In the first 3 hours of S phase we observed

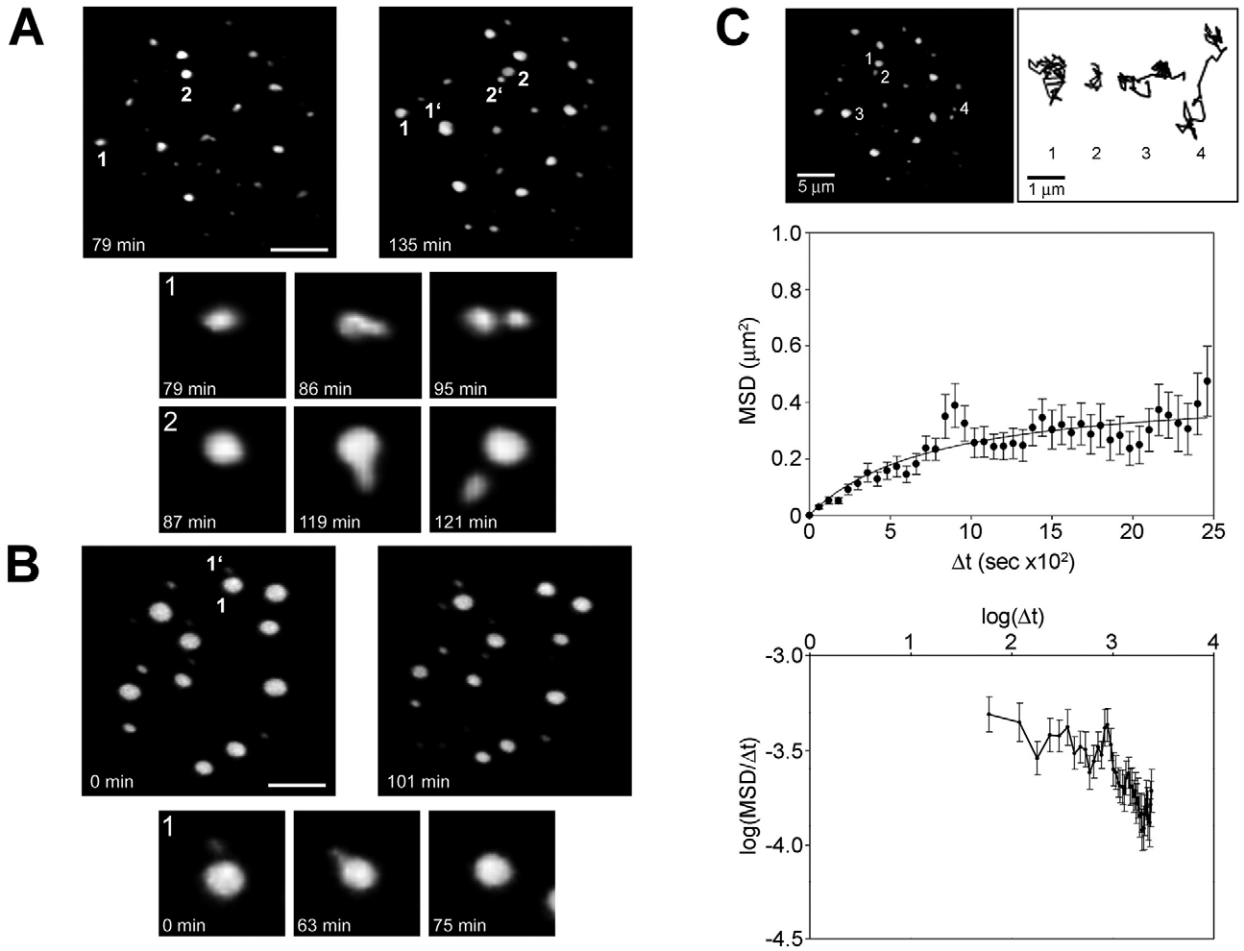

Fig. 2. Dynamics of PML nuclear bodies and PML protein in S phase. (A) U-2 OS cells expressing GFP-PML IV were imaged for 2 hours in early S phase, during which several fission events were observed. Two fission events are shown in the bottom panel (1 and 2). The resulting microbodies are labelled 1' and 2'. (B) During a similar period supramolecular fusion events were also observed (labelled 1), shown in more detail in the bottom panel. The microbody that fuses with the larger PML nuclear body is indicated as 1' in the left panel. (C) Relative movement of several PML nuclear bodies is shown (top panel, nuclear bodies 1-4). A mean square displacement (MSD) plot (middle panel) and a log(MSD/Δt) versus log(Δt) plot (bottom panel) describes the PML nuclear body movement (mean ± s.e.; n=57, over 45 minutes). Bar, 5 µm.

several supramolecular fission events (Fig. 2A; supplementary material Movie 1). These fission events were preceded by a prolonged period of extensive dynamic instability, culminating in the 'pulling away' or 'shearing' of the fission product (Fig. 2A panels 1 and 2; supplementary material Movie 2). The proportion of PML nuclear bodies that undergo fission vary from 30% to 90% depending on where the cells are in S phase during imaging. Although we also observed fusion events between nascent bodies and parental PML nuclear bodies (Fig. 2B panel 1, supplementary material Movie 3), more fission events than fusion events account for the net increase in PML nuclear body number during early S phase.

We observed that the relative sizes of PML nuclear bodies at the beginning of S phase varied widely. The fission product, however, was often significantly smaller in size than the parental PML nuclear body (Fig. 2A). As the cell progressed through S phase and into G2, the fission products and the parental PML nuclear bodies become more uniform in size (supplementary material Fig. S2) through a redistribution of PML protein between the bodies and the nucleoplasm. This is consistent with our FRAP data which indicate that the PML protein exchanges at a higher rate with the nucleoplasm in S phase than in G1 of the cell cycle (supplementary material Fig. S4). Thus, such an exchange of PML protein might explain how nascent PML microbodies increase in size by G2.

PML is redistributed from a protein core to chromatin fibres in early S phase

The dynamic instability leading to fission of PML nuclear bodies in early S phase implies exposure to physical forces, perhaps generated from an underlying nuclear protein architecture or from connections to chromatin. Previously, we have shown by correlative fluorescence and electron spectroscopic imaging (ESI) that the cores of PML nuclear bodies are radially symmetric spheres or cylinders composed of protein, and anchored in place by multiple contacts with the surrounding chromatin (Boisvert et al., 2000; Eskiw et al., 2004; Eskiw et al., 2003). To understand the basis for their

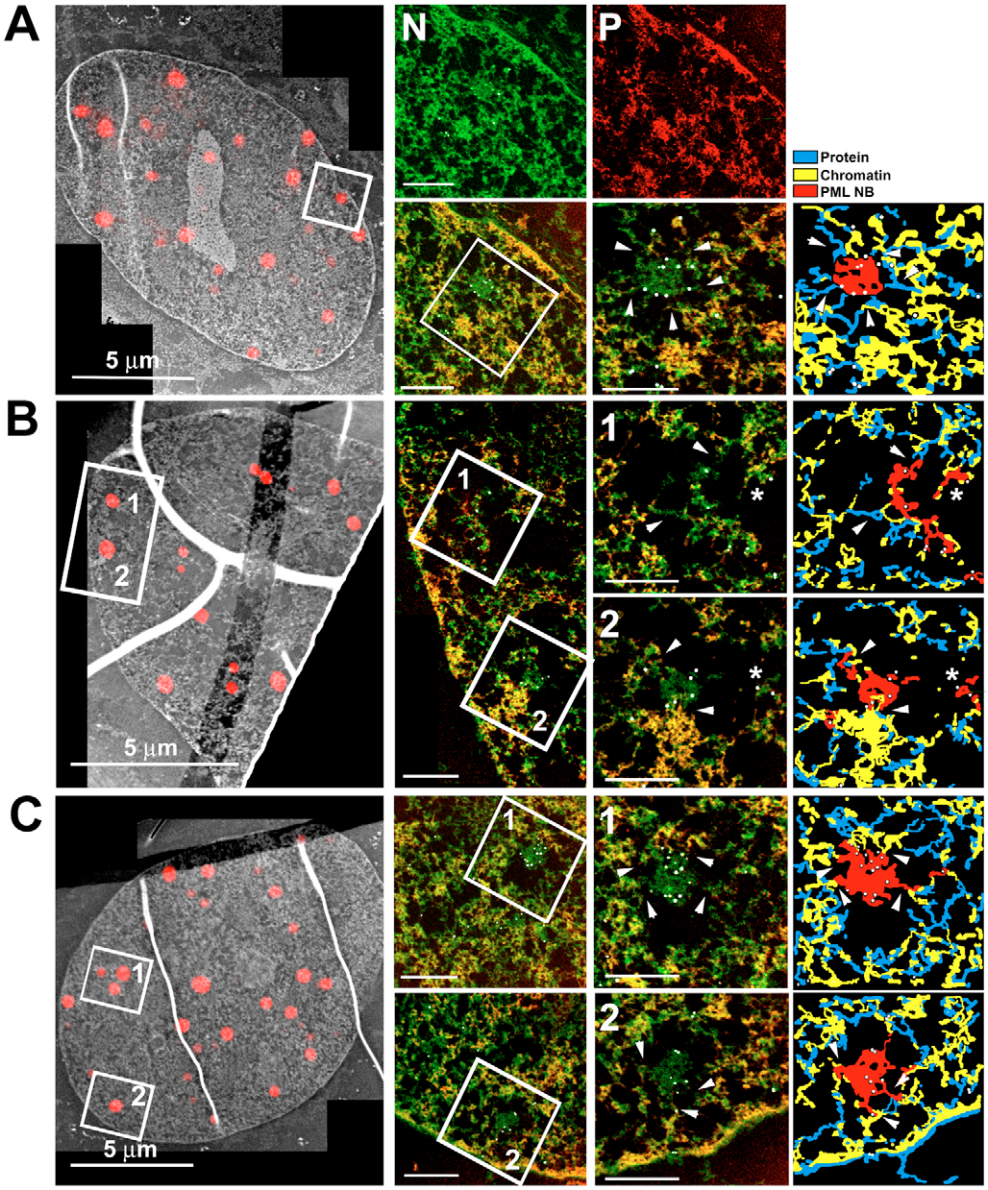

Fig. 3. Ultrastructural analysis of PML nuclear bodies in S phase by correlative LM/ESI. (A) Correlative fluorescence and electron microscopy of a G2 cell, fluorescently labelled for PML protein. Elemental maps of nitrogen (N) and phosphorus (P), and the merged maps of a PML nuclear body and its surrounding nucleoplasm reveal protein-based (green) and nucleic-acid-based (red) components. Chromatin appears yellow in the merged image because of its high N and P content. A field is shown at higher magnification. The imaged PML nuclear body (right hand panel, red) makes extensive contacts (white arrowheads) with the surrounding chromatin (yellow) directly and through non-chromosomal protein (blue) contacts. (B) Electron micrographs of PML nuclear bodies in an early S phase cell. PML microbodies are indicated by white asterisks and chromatin contacts by white arrowheads. (C) Electron micrographs of PML nuclear bodies in a mid S phase cell. Chromatin contacts are indicated by white arrowheads. Bars, 500 nm.

apparent structural instability in early S phase, we applied correlative fluorescence and ESI to characterise the ultrastructure of both PML nuclear bodies and the surrounding chromatin (Fig. 3). In this way, we hoped to determine if the observed increase in PML nuclear body dynamics is indeed related to changes in the interaction between chromatin and these bodies.

Samples were prepared as they would be for conventional transmission electron microscopy and ESI was used to generate nitrogen and phosphorus maps (Fig. 3) (Dellaire et al., 2004). Since nitrogen maps (green) contrast both protein and nucleic acid and phosphorus (red) primarily contrasts nucleic acids, the ratio of the nitrogen and phosphorus levels is used to distinguish non-chromosomal protein structures such as PML nuclear bodies (green) from chromatin (yellow). The position of the body was determined by correlating the immunofluorescence localisation of PML in the physical section with the low magnification electron micrograph of the same section. Immunogold detection was also used to delineate the location of PML protein within the structure identified by correlative fluorescence microscopy and electron spectroscopic imaging. Continuous protein structures that contain a gold particle (Fig. 3, white dots) were considered a part of the PML nuclear body. In G1 and G2, PML nuclear bodies have a radially symmetric protein core, which makes several contacts with the surrounding chromatin (e.g. G2 cell shown in Fig. 3A, white arrows). By contrast, the PML nuclear bodies in early S phase are clearly disrupted, often retaining no radial symmetry (Fig. 3B). Instead of a compact protein-based core with chromatin connections at its periphery, the PML protein is more dispersed and spread along chromatin fibres (Fig. 3B, white arrows). This subset of PML accumulations, which appear to be spheres by light microscopy, can no longer be described morphologically as 'bodies' but still retain intimate contacts with chromatin. Therefore, rather than chromatin contact being broken, they are continually maintained but the integrity of the body is compromised. Large spaces are also seen between the chromatin fibres and between the protein-based remnants of the bodies. Small PML-containing protein structures are also observed in early S phase that may represent fission products from the adjacent PML nuclear body (Fig. 3B, white asterisks). The unique PML nuclear body structure in cells overexpressing the PML I isoform dramatically illustrates the elongation and duplication of PML nuclear bodies seen in early S phase (supplementary material Fig. S5). As cells progress into mid S phase, the interchromatin domain space around the PML nuclear body begins to decrease in size, correlating with the re-formation of a protein-based core as the chromatin at the periphery of the bodies returns to a topological state seen before S phase (Fig. 3C, white arrows; summarised in Fig. 4). In addition, doublets of PML nuclear bodies in close proximity to each other are frequently observed after mid S phase by both light (Fig. 1D) and electron microscopy (supplementary material Fig. S5).

To further relate the loss of structural integrity of PML nuclear bodies in early S phase to changes in chromatin contacts, we transiently expressed PML$^{-/-}$ MEFs with either GFP-PML IV or GFP-PML IV-3K (lacking SUMO-1 modification sites). PML nuclear bodies formed with this mutated form of PML lack the proteins normally associated with bodies, including adaptors for contacts with chromatin

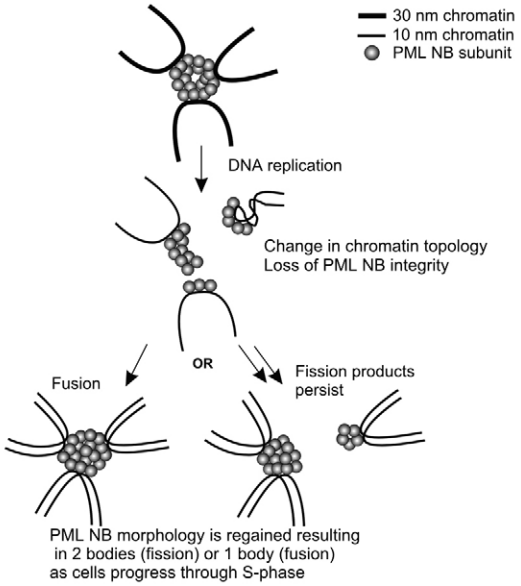

Fig. 4. Model for PML nuclear body (NB) replication in S phase. In early S phase, chromatin pulls PML nuclear bodies apart as changes occur in chromatin topology, related to replication. Some microbodies may fuse with each other or with the parental bodies, with a net increase in PML nuclear body number of up to twofold.

(Zhong et al., 2000). We then treated these transfected cells with actinomycin D. Previously we showed that the structural integrity of the PML nuclear body was affected by actinomycin D treatment, through changes in chromatin condensation and/or DNA damage (Eskiw et al., 2004). These changes were not sensitive to the overexpression of SUMO-1, suggesting that this mechanism of PML nuclear body disruption was independent of the loss of SUMO-1 from PML. We observed the formation of microstructures in MEFs expressing GFP-PML IV but not in MEFs expressing GFP-PML IV-3K (supplementary material Fig. S6). Although this mechanism of body disruption is insensitive to SUMO-1 overexpression (Eskiw et al., 2004), SUMO-1 modification of PML is required for the fission of PML microbodies in response to changes in chromatin structure, presumably because the connections made between PML nuclear bodies and chromatin through adaptors are dependent on sumolyated PML protein. This observation strengthens our interpretation of the live-cell and ESI data, that the structural instability and fission seen in S phase is related to changes in the relationship between chromatin and PML nuclear bodies.

Mobility of fission products of PML nuclear bodies is consistent with attachments to chromatin

PML nuclear bodies are relatively immobile within the nucleus during extended periods of interphase (supplementary material Movie 4) (Eskiw et al., 2004; Eskiw et al., 2003; Wiesmeijer et al., 2002). We characterised the mobility of PML-containing structures in S phase in U-2 OS cells expressing GFP-PML IV (Fig. 2C). After adjusting for cell drift that occurred during imaging, the movement of the majority of PML nuclear bodies observed in S phase was confined to an oscillation of one to two body diameters (Fig. 2C, PML nuclear bodies 1 to 3). In addition, many of the new bodies that formed during our

analysis remained in the immediate vicinity of the parental body from which they were derived (supplementary material Movie 1). A minority of new bodies, although similarly constrained to a defined nuclear volume, were capable of larger-scale movements of 2-3 μm (e.g. Fig. 2C, PML nuclear body 4). To confirm that PML nuclear body movement in S-phase cells was indeed constrained we plotted the mean square displacement (MSD) of these bodies over a time interval of 40 minutes (Fig. 2C), applying the methods described previously (Chubb et al., 2002). From the MSD plot we derived a diffusion constant of approximately 1.0×10^{-4} μm^2/second for PML nuclear bodies in S phase, equivalent to the diffusional mobility of chromatin in human cells (1.4×10^{-4} μm^2/second) (Chubb et al., 2002). This is consistent with the ESI results, showing that PML accumulations are associated with chromatin fibres. In addition, the movement of these fission products is consistent with anomalous diffusion, as the plot of log(MSD/Δt) versus log (Δt) for PML nuclear bodies in S phase results in a line with a negative slope (Fig. 2C). Our interpretation is that the PML nuclear body fission products and body remnants diffuse with the associated chromatin fibres. As these chromatin fibres diffuse, the PML accumulations may transiently associate with other chromatin fibres with which they come in contact, accounting for the anomalous nature of the diffusion.

The fission products are biochemically similar to the parental PML nuclear bodies

The structural instability of PML nuclear bodies in early S phase may result from a physical disruption of chromatin attachments with the PML nuclear bodies. Topological changes in chromatin, for example, could lead to chromatin pulling away from the body, pulling portions of the body away in the process. Alternatively, or in parallel, biochemical changes in the PML nuclear bodies may be required to permit the fission process. To test this possibility, we compared the SUMO-1 and Sp100 levels of the fission products with PML nuclear bodies in asynchronous cells. The biochemistry of all PML-containing bodies did not change with respect to SUMO-1 and Sp100 content at all time points in S phase (supplementary material Fig. S7). Similar observations were made in normal human fibroblasts (GM05757) and SK-N-SH cells (data not shown). Therefore, nascent PML nuclear bodies in early S phase continue to contain SUMO-1, and as a consequence, are competent for fusion with other PML nuclear body fission products or with the parental bodies (Eskiw et al., 2003). We conclude that the basis for PML nuclear body structural instability is primarily biophysical, based on changes in chromatin topology, rather than on intrinsic biochemical alterations, such as SUMO-1 modifications.

Discussion

PML nuclear body integrity and chromatin interactions

Although PML nuclear bodies appear to play a role in many nuclear events, how they function is not known. One model is that PML nuclear bodies are discrete structures that can diffuse and ricochet off structures in the nucleoplasm. These spheres of PML together with other associated proteins are thought to act as depots, which may have no direct or indirect relationship to chromatin. They may be considered as sites of excess nuclear protein and/or sites of accumulation of multi-subunit protein complexes that participate in various post-translational modifications of nuclear factors. A second model is that specific chromosome loci associate with the bodies, so that their position in the nucleus is non-random and some degree of tethering to chromatin may occur (reviewed by Ching et al., 2005).

Previously, we have shown that the structural stability of PML nuclear bodies is dependent on the state of chromatin integrity (Eskiw et al., 2004). In this paper, we provide support for a direct association of PML nuclear bodies with chromatin. In early S phase, when euchromatin is being replicated, PML nuclear bodies become structurally unstable, when visualised in live cells by fluorescence microscopy, and appear to break up by a fission mechanism, producing numerous fission products around the parental body. Because the fission products are mobile, they can frequently be seen to contact each other and fuse, or less frequently, fuse with the parental PML nuclear bodies. The final result on average is that between 1.3 and 2 (depending on the cell type) new PML nuclear bodies are observed where there was previously only one. This result provides a link between the structural stability of PML nuclear bodies and chromatin replication. More importantly, however, we show that chromatin and PML have an even more intimate relationship than previously thought. In interphase, the core of the PML nuclear body is, on average, a ~300 nm diameter sphere of protein which makes contacts with the surrounding chromatin (Eskiw et al., 2003). During this period of PML nuclear body instability in early S phase, however, the PML protein is no longer assembled into a tight protein core, when viewed at the ultrastructural level (Fig. 3). Instead, the PML protein becomes redistributed along 10 and 30 nm chromatin fibres within a region up to a few hundred nanometers in diameter. It is this redistribution along chromatin fibres that gives the impression of fission of the nuclear body. In fact, the 'body' itself, i.e. as a sphere of PML and associated proteins, no longer exists during this transient period. We suggest that as topological changes occur in the replicating chromatin, the chromatin that contacted the bodies retracts away from the bodies, thereby pulling the bodies apart. Although PML protein probably does not bind directly to DNA, other proteins found in PML nuclear bodies that can bind chromatin may act as adaptors. The expression in PML-null fibroblasts of a mutant form of PML IV, lacking the acceptor lysines for sumoylation, results in the formation of large aggregates of PML rather than PML nuclear bodies. These structures fail to recruit chromatin adaptors (PML-IV 3K, supplementary material Fig. S6) (Zhong et al., 2000). Whereas fission into microbodies occurred in the presence of wild-type PML IV, microbodies did not form in cells expressing the mutant PML IV in S phase, presumably owing to the loss of these chromatin adaptors (supplementary material Fig. S6). Therefore it is unsurprising that PML nuclear bodies, which remain sumoylated throughout interphase and would be expected to maintain their complement of chromatin adaptor proteins (supplementary material Fig. S7), are disrupted during S phase when chromatin undergoes considerable topological change.

Although the majority of new PML nuclear bodies in early S phase arise from supramolecular fission, it is possible that some PML nuclear bodies may nucleate de novo as proposed for the redistribution of PML nuclear bodies following HSV-1 infection (Everett and Murray, 2005; Everett et al., 2004).

Although the new PML nuclear bodies at sites of accumulation of the viral DNA may have formed from molecular PML in the nucleoplasm, future studies could be performed to determine whether the stress of the viral infection could also cause disruption of bodies by a fission mechanism.

Whereas we have not observed significant PML nuclear body mobility in cells outside of S phase (Eskiw et al., 2004), we do observe that the PML nuclear body fission products diffuse at the same rate as euchromatin (Fig. 2C) (Chubb et al., 2002). By contrast, others have shown that PML nuclear bodies can diffuse in the interchromatin domain space with diffusion constants much higher than chromatin (Gorisch et al., 2004). A 'Moving corral model' was developed to explain the dynamics of PML nuclear bodies, in which they are considered as discrete entities enclosed within a 'chromatin corral', and in which they can diffuse. Although we agree that there is an inter-relationship between the ICD space and the diffusional mobility of PML-containing structures (Eskiw et al., 2003; Gorisch et al., 2004), our study of the dynamic behaviour of PML nuclear bodies in S phase and in mitosis (Dellaire et al., 2006) also suggests that contacts between PML nuclear bodies and the surrounding chromatin can contribute to both the integrity and diffusional characteristics of these supramolecular assemblies within the nucleus. Since Gorisch and colleagues did not specifically control for cell cycle-dependent changes in PML nuclear body dynamics, it is almost certain that a significant proportion of the cells they observed where in S phase and actively replicating their DNA (Gorisch et al., 2004), which might explain the increased mobility of PML nuclear bodies reported in their study. Alternatively or in addition, the observed differences between the mobility of PML nuclear bodies in their study and ours may reflect different imaging conditions between the studies. In particular, DNA damage (Eskiw et al., 2004) or photo-toxic stress acquired during imaging could have an affect on PML nuclear body integrity and behaviour. Clearly, any future study on the mobility of PML nuclear bodies will have to take in account both the cell cycle state of the cells observed and the specific imaging conditions used.

What are the functional consequences of an increase in PML nuclear body number in S phase?

PML nuclear bodies increase in number by up to twofold by a mechanism of supramolecular fission in early S phase (Fig. 4). This increase may provide clues for the function of PML nuclear bodies. We have proposed that PML nuclear bodies may be sites of nuclear activity where the PML nuclear bodies service the neighbouring chromatin domains (Boisvert et al., 2000; Ching et al., 2005). An increase in PML nuclear body number predominately in early S phase (Fig. 1B and supplementary material Fig. S2) indirectly supports this model and suggests that PML nuclear bodies are primarily associated with euchromatin rather than heterochromatin, which replicates late in S phase. An increase in the number of euchromatin domains would thereby require an increase in the number of PML nuclear bodies.

Newly formed PML nuclear bodies in S phase could also function to maintain chromosomal domain order, such as spatially orienting sister chromatids prior to prophase. Interestingly, PML$^{-/-}$ mice that lack PML nuclear bodies exhibit higher rates of sister-chromatid exchange, characteristic of Bloom syndrome (Zhong et al., 1999). The Bloom syndrome protein (BLM), which localises to PML nuclear bodies at the G1-S boundary (Wang et al., 2001; Zhong et al., 1999), is thought to function in early-S-phase-specific surveillance of both replication fork collapse and of DNA adducts that block replication fork progression (Pichierri et al., 2004). Therefore, nascent PML nuclear bodies containing the BLM protein may form by fission events in early S phase to function transiently in the surveillance of replication fork collapse and then fuse back with parental PML nuclear bodies as S phase progresses. We are currently examining these possibilities.

Materials and Methods

Cell culture

SK-N-SH cells and PML$^{-/-}$ MEFs (a generous gift from P. P. Pandolfi, Memorial Sloan-Kettering Cancer Center, New York, NY) were grown in DMEM (Wisent) supplemented with 10% FBS (Wisent), 10 μg/ml penicillin and streptomycin (Sigma), and 2 mM L-glutamine (Sigma). U-2 OS stably expressing GFP-PML IV (a gift from J. Taylor, Medical College of Wisconsin, Milwaukee, WI) were grown in DMEM supplemented with 10% FBS, 10 μg/ml penicillin and streptomycin, 1600 μg/ml G418 (Wisent), and 2 mM L-glutamine. GM05757 cells were cultured in alpha-MEM (Wisent) supplemented with 15% FBS, 10 μg/ml penicillin and streptomycin, and 2 mM L-glutamine. Cells were synchronised at the G1-S border with media (DMEM or α-MEM) containing 10% FBS and 5 μg/ml aphidicolin (Sigma) for 24 hours at 37°C. Cells were released from aphidicolin arrest by rinsing cells three times with PBS, followed by the addition of fresh culture medium.

Immunofluorescence microscopy and BrdU labelling

Cells were prepared for immunolabelling as described (Eskiw et al., 2003). To label with BrdU, cells were pulsed with 20 μM BrdU for 30 minutes, fixed in methanol for 30 minutes at –20°C. The methanol was removed and 4N HCl was added to the cells for 2 minutes at room temperature (RT). Cells were washed three times with PBS at RT. Primary antibodies used were: PML, mAb 5E10 (a gift from R. van Driel, University of Amsterdam, The Netherlands), AB1370 (Chemicon); Sp100, AB1380 (Chemicon); Cyclin A, sc-751 (Santa Cruz); SUMO-1, mAb 21C7 (Zymed); BrdU, mAb B44 (BD Biosciences). Secondary antibodies used were donkey anti-mouse or rabbit Cy3 and Cy5 (Jackson Laboratories). For electron microscopy, donkey anti-mouse conjugated with Ultrasmall Gold (Electron Microscopy Sciences) was used. For fluorescence microscopy, coverslips were mounted on glass slides using 90% glycerol/PBS containing 1 mg/ml paraphenlenediamine and 1 μg/ml 4′,6-Diamidino-2-phenylindole (DAPI). Images were collected on a Leica Microsystems DMRA2 upright microscope equipped with a Hamamatsu ORCA-ER camera using the 63× 1.32 NA oil-immersion objective. OpenLab 3.5.1 (Improvision) software was used to collect images, and the images were processed with Photoshop 7.0 (Adobe). Line scans were performed using ImageJ (NIH) software.

Live-cell imaging and particle tracking

Live-cell imaging of U-2 OS cells was performed using RPMI media (Wisent) supplemented with 10% FBS at 37°C. Images were acquired using a Leica DMIRE2 inverted microscope equipped with a Hamamatsu ORCA-AG camera, a Wave FX spinning disk confocal unit (Quorum Technologies), and an argon ion laser (Melles Griot). Image stacks were taken once every minute for 60 minutes. OpenLab 3.5.1 (Improvision) software was used to collect 4D stacks. Images were processed with Photoshop 7.0 (Adobe). Particle tracking was performed using Volocity (Improvision). MSD analysis was performed as described (Chubb et al., 2002; Platani et al., 2002).

For cell cycle progression experiments, DIC images of SK-N-SH cells were acquired hourly for 16 hours with a Leica DMRA2 upright fluorescence microscope. Cells were then fixed and immunolabelled for PML and cyclin A.

DNA constructs and transient transfections

The pDiHcRed-PCNA was constructed by cloning PCNA from pYFP-PCNA (a gift from J.R. Chubb, University of Dundee, UK) into pDiHcRed. The pCDNA-GFP-PML IV-3K was constructed by cloning GFP into pBABE-PML IV-3K (a gift from O. Bischof, Institute Pasteur, Paris, France), and cloning GFP-PML IV-3K into pCDNA 3.1. For transient transfections lipofectamine 2000 (Invitrogen) was used as instructed.

Western analysis

Cells were grown in six-well dishes and 2× SDS-PAGE loading buffer was added to the cells. For the G1-phase sample, cells were grown to confluency and left to culture for 2 days. For the S-phase sample, cells were grown to confluency,

trypsinised, and replated into a well with medium containing 5 μg/ml aphidicolin for 24 hours. Cells were released from the aphidicolin arrest for 2 hours. For the G2-phase sample, cells were arrested in the same manner as the S-phase sample, but cells were released from the aphidicolin arrest for 8 hours. Protein samples were separated by 10% SDS-PAGE and transferred onto nitrocellulose (Amersham Biosciences). PML and actin protein was detected using rabbit anti-PML (AB1370, Chemicon) and mouse anti-actin (Sigma) antibodies. Secondary labeling was conducted using goat anti-rabbit HRP (Cell Signaling) and goat anti-mouse HRP (Sigma). Bands were detected using an ECL kit and quantified using FluorChem 2.0 (Alpha Innotech Corporation) software.

Flow cytometry

Cells were harvested and pelleted. The pellet was resuspended in 50 μl HBSS with 2% FBS. Cells were fixed with 1 ml ice-cold 80% ethanol for 30 minutes on ice. Cells were pelleted and resuspended in HBSS containing 0.1 mg/ml propidium iodide (Sigma) and 0.6% NP-40 to final concentration of 2×10^6 cells/ml. An equal volume of 2 mg/ml RNase in HBSS was added and incubated at room temperature in the dark for 30 minutes. This solution was then filtered through a 40 μm nylon mesh (BD Biosciences) and keep on ice until analysis. Cells were analyzed on a FACscan flowcytometer (BD Biosciences). Data analysis was performed using FlowJo 6.0 (Tree Star).

Fluorescence recovery after photobleaching (FRAP)

FRAP was performed on the Leica LSM 510 confocal microscope system equipped with an argon ion laser source at 488 nm using a 63× 1.32 NA oil-immersion objective at 37°C. To determine the shortest length of time needed to bleach a PML nuclear body, PML nuclear bodies from fixed cells were bleached. For FRAP experiments, 10-12 confocal sections were acquired followed by five bleach pulses per confocal slice at 25% power and 100% transmittance for total time of 0.8 seconds. Images of confocal stacks were collected of the bleached PML nuclear body and a reference PML nuclear body every 30 seconds at 5% transmittance. Images of multiple sections were collected at time intervals of 30 seconds. Quantitative analysis of the amount of fluorescence in bleached regions relative to unbleached regions was performed with ImageJ (NIH) software. Corrections were made for fluorescence fading that occurred during imaging.

Correlative microscopy and electron spectroscopic imaging (ESI)

Following immunolabelling, cells were prepared by the standard methods used for conventional transmission electron microscopy (TEM) and electron spectroscopic imaging (ESI) was performed (Dellaire et al., 2004). Electron micrographs were taken at 200 kV on a transmission electron microscope (Tecnai 20, FEI). Energy filtered images were collected using a post-column imaging filter (Gatan) as described elsewhere (Dellaire et al., 2004).

We thank O. Bischof for the pBABE-PML IV-3K plasmid, P.P. Pandolfi for the PML$^{-/-}$ MEFs, and Ren Li for ESI assistance. G.D. is a Senior Postdoctoral Fellow of the Canadian Institutes of Health Research (CIHR). R.W.C. is a recipient of a Restracomp Studentship from The Hospital for Sick Children Research Institute. This work was supported by an operating grant from the CIHR (MOP-64405) to D.P.B.-J. D.P.B.-J. is the recipient of the Canada Research Chair in Molecular and Cellular Imaging.

References

Bernardi, R. and Pandolfi, P. P. (2003). Role of PML and the PML-nuclear body in the control of programmed cell death. *Oncogene* **22**, 9048-9057.

Boisvert, F. M., Hendzel, M. J. and Bazett-Jones, D. P. (2000). Promyelocytic leukemia (PML) nuclear bodies are protein structures that do not accumulate RNA. *J. Cell Biol.* **148**, 283-292.

Chang, K. S., Fan, Y. H., Andreeff, M., Liu, J. and Mu, Z. M. (1995). The PML gene encodes a phosphoprotein associated with the nuclear matrix. *Blood* **85**, 3646-3653.

Ching, R. W., Dellaire, G., Eskiw, C. H. and Bazett-Jones, D. P. (2005). PML bodies: a meeting place for genomic loci? *J. Cell Sci.* **118**, 847-854.

Chubb, J. R., Boyle, S., Perry, P. and Bickmore, W. A. (2002). Chromatin motion is constrained by association with nuclear compartments in human cells. *Curr. Biol.* **12**, 439-445.

Dellaire, G. and Bazett-Jones, D. P. (2004). PML nuclear bodies: dynamic sensors of DNA damage and cellular stress. *BioEssays* **26**, 963-977.

Dellaire, G., Nisman, R. and Bazett-Jones, D. P. (2004). Correlative light and electron spectroscopic imaging of chromatin in situ. *Methods Enzymol.* **375**, 456-478.

Dellaire, G., Eskiw, C. H., Dehgani, H., Ching, R. W. and Bazett-Jones, D. P. (2006). Mitotic accumulations of PML protein contribute to the re-establishment of PML nuclear bodies in G1. *J. Cell Sci.* **119**, 1034-1042.

Drouin, A., Schmitt, A., Masse, J. M., Cieutat, A. M., Fichelson, S. and Cramer, E. M. (2001). Identification of PML oncogenic domains (PODs) in human megakaryocytes. *Exp. Cell Res.* **271**, 277-285.

Erlandsson, F., Linnman, C., Ekholm, S., Bengtsson, E. and Zetterberg, A. (2000). A detailed analysis of cyclin A accumulation at the G(1)/S border in normal and transformed cells. *Exp. Cell Res.* **259**, 86-95.

Eskiw, C. H., Dellaire, G., Mymryk, J. S. and Bazett-Jones, D. P. (2003). Size, position and dynamic behavior of PML nuclear bodies following cell stress as a paradigm for supramolecular trafficking and assembly. *J. Cell Sci.* **116**, 4455-4466.

Eskiw, C. H., Dellaire, G. and Bazett-Jones, D. P. (2004). Chromatin contributes to structural integrity of promyelocytic leukemia bodies through a SUMO-1-independent mechanism. *J. Biol. Chem.* **279**, 9577-9585.

Everett, R. D. (2001). DNA viruses and viral proteins that interact with PML nuclear bodies. *Oncogene* **20**, 7266-7273.

Everett, R. D. and Murray, J. (2005). ND10 components relocate to sites associated with herpes simplex virus type 1 nucleoprotein complexes during virus infection. *J. Virol.* **79**, 5078-5089.

Everett, R. D., Sourvinos, G., Leiper, C., Clements, J. B. and Orr, A. (2004). Formation of nuclear foci of the herpes simplex virus type 1 regulatory protein ICP4 at early times of infection: localization, dynamics, recruitment of ICP27, and evidence for the de novo induction of ND10-like complexes. *J. Virol.* **78**, 1903-1917.

Gorisch, S. M., Wachsmuth, M., Ittrich, C., Bacher, C. P., Rippe, K. and Lichter, P. (2004). Nuclear body movement is determined by chromatin accessibility and dynamics. *Proc. Natl. Acad. Sci. USA* **101**, 13221-13226.

Koken, M. H., Linares-Cruz, G., Quignon, F., Viron, A., Chelbi-Alix, M. K., Sobczak-Thepot, J., Juhlin, L., Degos, L., Calvo, F. and de The, H. (1995). The PML growth-suppressor has an altered expression in human oncogenesis. *Oncogene* **10**, 1315-1324.

Leonhardt, H., Rahn, H. P., Weinzierl, P., Sporbert, A., Cremer, T., Zink, D. and Cardoso, M. C. (2000). Dynamics of DNA replication factories in living cells. *J. Cell Biol.* **149**, 271-280.

Melnick, A. and Licht, J. D. (1999). Deconstructing a disease: RARalpha, its fusion partners, and their roles in the pathogenesis of acute promyelocytic leukemia. *Blood* **93**, 3167-3215.

Pichierri, P., Franchitto, A. and Rosselli, F. (2004). BLM and the FANC proteins collaborate in a common pathway in response to stalled replication forks. *EMBO J.* **23**, 3154-3163.

Platani, M., Goldberg, I., Lamond, A. I. and Swedlow, J. R. (2002). Cajal body dynamics and association with chromatin are ATP-dependent. *Nat. Cell Biol.* **4**, 502-508.

Terris, B., Baldin, V., Dubois, S., Degott, C., Flejou, J. F., Henin, D. and Dejean, A. (1995). PML nuclear bodies are general targets for inflammation and cell proliferation. *Cancer Res.* **55**, 1590-1597.

Wang, J., Shiels, C., Sasieni, P., Wu, P. J., Islam, S. A., Freemont, P. S. and Sheer, D. (2004). Promyelocytic leukemia nuclear bodies associate with transcriptionally active genomic regions. *J. Cell Biol.* **164**, 515-526.

Wang, X. W., Tseng, A., Ellis, N. A., Spillare, E. A., Linke, S. P., Robles, A. I., Seker, H., Yang, Q., Hu, P., Beresten, S. et al. (2001). Functional interaction of p53 and BLM DNA helicase in apoptosis. *J. Biol. Chem.* **276**, 32948-32955.

Wiesmeijer, K., Molenaar, C., Bekeer, I. M., Tanke, H. J. and Dirks, R. W. (2002). Mobile foci of Sp100 do not contain PML: PML bodies are immobile but PML and Sp100 proteins are not. *J. Struct. Biol.* **140**, 180-188.

Zhong, S., Hu, P., Ye, T. Z., Stan, R., Ellis, N. A. and Pandolfi, P. P. (1999). A role for PML and the nuclear body in genomic stability. *Oncogene* **18**, 7941-7947.

Zhong, S., Muller, S., Ronchetti, S., Freemont, P. S., Dejean, A. and Pandolfi, P. P. (2000). Role of SUMO-1-modified PML in nuclear body formation. *Blood* **95**, 2748-2752.